Title

The SUN protein UNC-84 is required only in force-bearing cells to maintain nuclear envelope architecture

Journal

Journal of Cell Biology, 206(2)

ISSN

0021-9525

Authors

Cain, Natalie E
Tapley, Erin C
McDonald, Kent L
et al.

Publication Date

2014-07-21

DOI

10.1083/jcb.201405081

Peer reviewed

The SUN protein UNC-84 is required only in force-bearing cells to maintain nuclear envelope architecture

Natalie E. Cain,[1] Erin C. Tapley,[1] Kent L. McDonald,[3] Benjamin M. Cain,[2] and Daniel A. Starr[1]

[1]Department of Molecular and Cellular Biology and [2]Department of Physics, University of California, Davis, Davis, CA 95616
[3]Electron Microscope Laboratory, University of California, Berkeley, Berkeley, CA 94720

The nuclear envelope (NE) consists of two evenly spaced bilayers, the inner and outer nuclear membranes. The Sad1p and UNC-84 (SUN) proteins and Klarsicht, ANC-1, and Syne homology (KASH) proteins that interact to form LINC (linker of nucleoskeleton and cytoskeleton) complexes connecting the nucleoskeleton to the cytoskeleton have been implicated in maintaining NE spacing. Surprisingly, the NE morphology of most *Caenorhabditis elegans* nuclei was normal in the absence of functional SUN proteins. Distortions of the perinuclear space observed in *unc-84* mutant muscle nuclei resembled those previously observed in HeLa cells, suggesting that SUN proteins are required to maintain NE architecture in cells under high mechanical strain. The UNC-84 protein with large deletions in its luminal domain was able to form functional NE bridges but had no observable effect on NE architecture. Therefore, SUN-KASH bridges are only required to maintain NE spacing in cells subjected to increased mechanical forces. Furthermore, SUN proteins do not dictate the width of the NE.

Introduction

The nuclear envelope (NE) is composed of two lipid bilayers, the inner nuclear membrane (INM) and outer nuclear membrane (ONM). The ONM is continuous with the ER membrane, and the INM and ONM are connected to each other at nuclear pores. Between the nuclear pores, the INM and ONM are separated by a uniform space of 30–50 nm, called the perinuclear space (PNS), which is connected to the ER lumen (Franke et al., 1981). How the even spacing of the INM and ONM is established and maintained is poorly understood.

A previous study leads to our central hypothesis that linker of nucleoskeleton and cytoskeleton (LINC) complexes regulate NE architecture (Crisp et al., 2006). LINC complexes are formed through the interaction of INM Sad1 and UNC-84 (SUN) proteins and ONM Klarsicht, ANC-1, and Syne homology (KASH) proteins in the PNS (Padmakumar et al., 2005; Crisp et al., 2006; McGee et al., 2006; Sosa et al., 2012). SUN and KASH proteins form NE bridges to transfer forces generated in the cytoplasm to the nucleoskeleton (Starr and Fridolfsson, 2010). The role of LINC complexes in the spacing of the NE in HeLa cells was tested by disrupting LINC complexes and examining NE ultrastructure. Either siRNA knockdown of *Sun1* and *Sun2* or expression of a dominant-negative SUN construct causes expansion of the PNS and blebbing of the ONM away from the INM (Crisp et al., 2006). HeLa and other tissue-culture cells adhered to a tissue-culture dish are, however, under heightened intracellular tension and mechanical strain (Wang et al., 2009a), and their nuclei are flattened (Magidson et al., 2011). The extent to which SUN-KASH bridges function to regulate NE architecture in the context of an in vivo tissue in a developing organism where most nuclei are close to spherical and subjected to presumably smaller mechanical forces remains unknown.

Here, we test the hypothesis that LINC complexes regulate NE architecture in vivo using *Caenorhabditis elegans* as a model. The SUN protein UNC-84 is expressed in *C. elegans* somatic cells after early embryogenesis, where it functions to move and anchor nuclei to specific intracellular locations (Malone et al., 1999; Lee et al., 2002). The other known SUN protein in *C. elegans*, SUN-1, functions in the germline and the early embryo

Correspondence to Daniel A. Starr: dastarr@ucdavis.edu

Abbreviations used in this paper: DIC, differential interference contrast; fps, frame per second; INM, inner nuclear membrane; KASH, Klarsicht, ANC-1, and Syne homology; LINC, linker of nucleoskeleton and cytoskeleton; NE, nuclear envelope; ONM, outer nuclear membrane; PNS, perinuclear space; SUN, Sad1p and UNC-84; TEM, transmission EM.

The Rockefeller University Press $30.00
J. Cell Biol. Vol. 206 No. 2 163–172
www.jcb.org/cgi/doi/10.1083/jcb.201405081

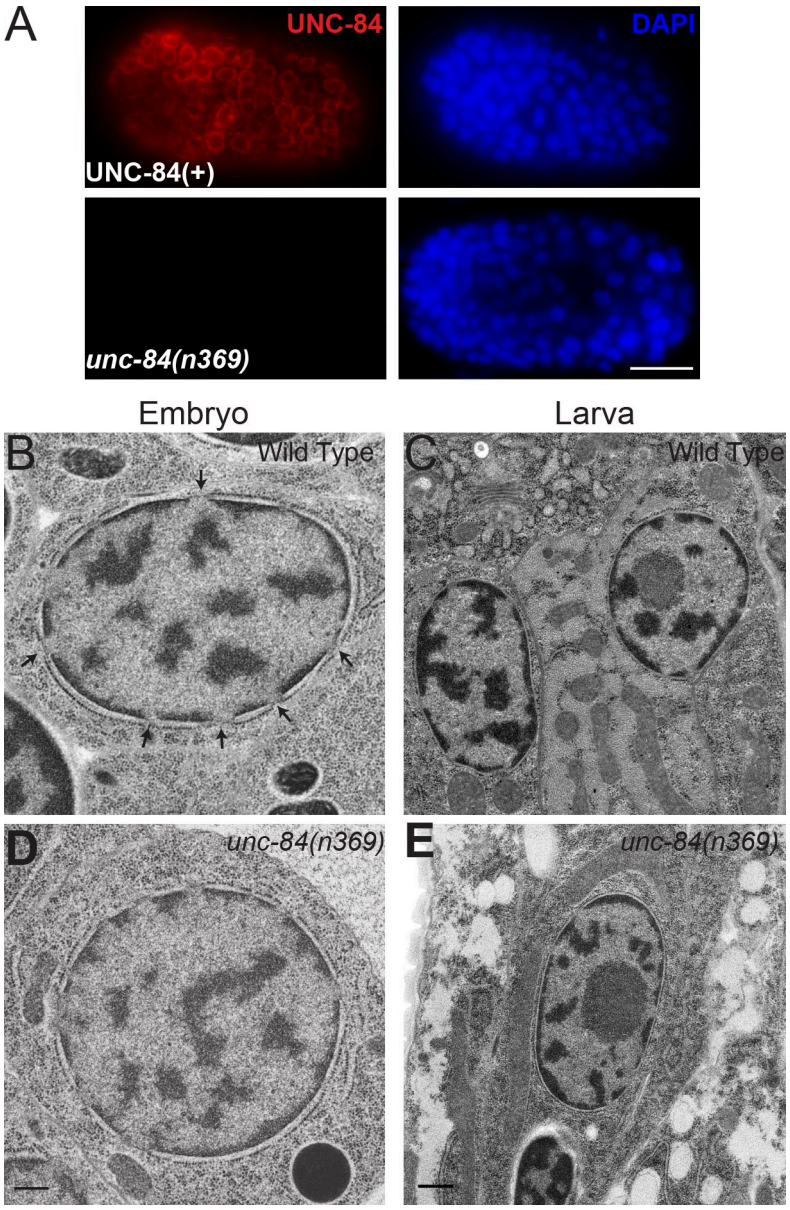

Figure 1. **Most nuclei in *unc-84(n369)* embryos and larvae display even spacing of the NE.** (A) UD87 (*unc-84(n369)* expressing the full-length UNC-84 rescuing fragment) and *unc-84(n369)* precomma stage embryos were stained with anti–UNC-84 antibodies. DAPI was used to stain nuclei. Bar, 10 µM. (B–E) Thin-section TEM was performed on wild-type (B and C) and *unc-84(n369)* (D and E) comma stage embryos (B and D) and L1 larvae (C [pharyngeal] and E [hypodermal]). Arrows indicate nuclear pores. Bars, 500 nm.

and is not expressed above detectable levels by immunofluorescence or serial expression of gene analysis (Fridkin et al., 2004; Minn et al., 2009; Wang et al., 2009b). In *unc-84(null)* mutant animals, both somatic KASH proteins UNC-83 and ANC-1 fail to localize to the ONM (Starr et al., 2001; Starr and Han, 2002; McGee et al., 2006). Despite a lack of somatic SUN-KASH bridges, *unc-84(null)* animals are viable, enabling us to perform quantitative EM of nuclear architecture in the absence of SUN-KASH bridges. Here, we show that NE spacing in most *unc-84(null)* cells was indistinguishable from wild type, and distortions of the type observed in HeLa cells were limited to body wall muscle nuclei. Furthermore, deleting most of the luminal domain of UNC-84 did not disrupt nuclear migration nor did it reduce the size of the PNS. Our results suggest that although LINC complexes are needed to maintain NE spacing in cells experiencing mechanical stress, they are dispensable otherwise, and they are insufficient to set the distance between the INM and ONM, as has been recently proposed (Sosa et al., 2013).

Results and discussion

UNC-84 is not required to maintain even NE spacing in most nuclei

To test the hypothesis that *unc-84(n369)* animals, which completely lack UNC-84 at the NE (Fig. 1 A), would display gross defects in NE architecture in a wide variety of *C. elegans* tissues, we performed transmission EM (TEM) to examine NE ultrastructure in wild-type and *unc-84(n369)* embryos and L1 larvae. Wild-type nuclei in premorphogenesis embryos (n = 57 nuclei) and L1 larvae (n = 50 hypodermal and pharyngeal cells examined, although many unidentifiable other cell types were also examined) displayed even spacing between the INM and ONM of ∼50 nm, as previously shown (Fig. 1, B and C; Cohen et al., 2002). Surprisingly, we found that *unc-84(n369)* nuclei were indistinguishable from wild type in embryos (Fig. 1 D is a representative image of 49/50 nuclei examined; one had what appeared to be an ER tubule attached to the ONM) and in the

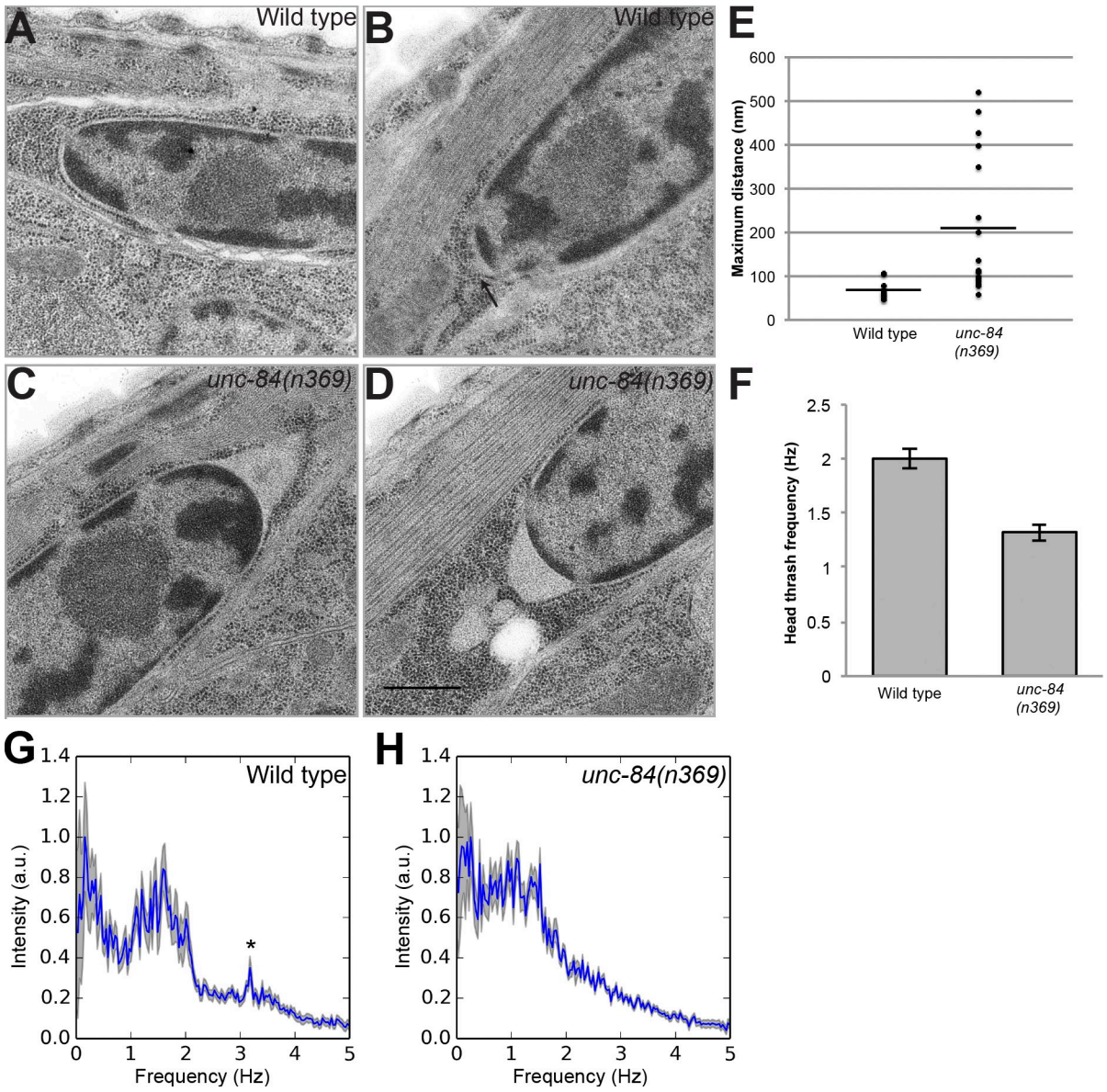

Figure 2. **Major NE distortions were observed in *unc-84(n369)* muscle nuclei.** (A–D) Representative thin-section TEM micrographs of L1 larval body wall muscles. (A and B) Wild-type nuclei with normal (A) and slightly distorted (B; arrow shows ~100-nm separation) nuclear membranes. (C and D) Large distortions were observed at the ends of *unc-84(n369)* nuclei. (E) Quantitation of the maximum PNS at the ends of ≥10 nuclei of each genotype. *unc-84(n369)* nuclei had a significantly larger mean space than wild type ($P = 0.0021$). The horizontal bars denote the mean values. Bar, 500 nm. (F) Mean frequency of head thrashing for wild-type and *unc-84(n369)* L1 larvae. Error bars are 95% confidence intervals assuming Poisson distribution. (G and H) Blue traces represent the mean motion spectra for wild type and *unc-84(n369)*; shaded regions represent standard deviation of the mean. The asterisk indicates the secondary harmonic peak. a.u., arbitrary unit.

hypodermis and pharynx of the larva (Fig. 1 E is a representative image of 45 nuclei examined). Because UNC-84 is required to recruit KASH proteins to the ONM (Starr et al., 2001; Starr and Han, 2002), *unc-84(n369)* nuclei lack SUN and KASH connections between the nucleoskeleton and cytoskeleton. Therefore, either LINC complexes do not function in NE architecture or nuclei in most tissues do not experience forces that disrupt the width of the PNS in the absence of SUN-KASH bridges.

Muscle nuclei in *unc-84* mutant animals display extreme NE distortion

We then focused our observations on larval body wall muscle nuclei, which were inferred to experience higher mechanical strain than other tissues and were therefore more likely to display NE architecture defects. Striated body wall muscles in *C. elegans* are rhomboid-shaped, mononucleated cells. Each cell is stretched along the anterior–posterior axis of the animal, the axis of contraction (Altun and Hall, 2009). Wild-type muscle nuclei were also greatly elongated along the long axis of the cell (Fig. 2). Muscle nuclei were therefore predicted to experience the largest mechanical strain at the anterior and posterior ends of the elongated nuclei, although no actual forces were measured in this study.

Most wild-type muscle nuclei displayed even NE spacing around the entire nucleus, including the ends (Fig. 2 A). Occasionally, the spacing between the INM and ONM widened

at the ends of the nuclei (Fig. 2 B shows the wild-type nucleus with the greatest observed PNS width). This supports the prediction that mechanical strain is greatest at the ends of muscle nuclei. In *unc-84(null)* muscle nuclei, large distortions of the NE were observed at the ends of the nuclei (Fig. 2, C and D). To quantify the extent of this irregular spacing, the point of widest separation between nuclear membranes (from multiple serial sections) for each body wall muscle nucleus was measured. In wild-type nuclei, the maximum distance between membranes ranged from 46.2 to 106.8 nm, with a mean of 68.1 nm (Fig. 2 E). In contrast, the maximum separation in *unc-84(null)* muscle nuclei ranged from 56.9 to 519.2 nm, with a mean of 209.4 nm (Fig. 2 E). ($n \geq 10$ and $P < 0.01$ in an unpaired two-tailed *t* test with Welch's correction between wild-type and *unc-84(n369)* muscle cells). Thus, the *unc-84(n369)* mutant displayed significantly wider NE spacing than wild type.

These data are consistent with the hypothesis that SUN and KASH bridges only play a role in maintaining the even spacing between the INM and ONM in cells under mechanical strain. Many human laminopathies disproportionately affect tissues, including skeletal and cardiac muscle, under high mechanical strain (Worman, 2012; Azibani et al., 2014). Mutations in both Nesprin-1 and SUN1 have been linked to striated muscle diseases, including Emery–Dreifuss muscular dystrophy and cardiomyopathy (Puckelwartz et al., 2010; Zhang et al., 2010; Li et al., 2014). To determine the extent to which *unc-84(n369)* mutants display locomotion defects that might be attributable to muscle defects, we filmed animals thrashing in liquid. L1 larvae were examined to eliminate the effect of neuronal defects caused by the loss of ventral cord neurons in older *unc-84* mutant animals with defects in P cell nuclear migration (Malone et al., 1999). Wild-type larvae thrashed on average at 2.0 ± 0.094 Hz (mean ± 95% confidence interval, n = 29), whereas *unc-84(n369)* larvae thrashed at 1.32 ± 0.075 Hz (mean ± 95% confidence interval, n = 30), a significant difference ($P = 0.0002$ in a two-sample Kolmogorov–Smirnov test; Fig. 2 F). Qualitatively, the wild-type larvae typically thrashed in relatively smooth sinusoidal patterns, whereas the *unc-84(n369)* larvae often twitched and coiled (Videos 1 and 2). To further characterize these differences, we performed spectral analyses of the videos. The mean motion spectrum for wild-type larvae showed a peak centered at 1.6 Hz extending up to 2 Hz, with a secondary peak (possibly a harmonic) at 3.2 Hz, indicating regular sinusoidal motion (Fig. 2 G). *unc-84(n369)* larvae exhibited a much broader spectrum of frequencies with a lower mean and no significant peaks, indicating more random motion (Fig. 2 H). These data are consistent with *unc-84(n369)* having a muscular defect potentially caused by the NE architecture defect. However, we cannot eliminate the possibility that this defect is caused by neuronal defects; the PVQ neuron is slightly mispositioned in ∼15% of *unc-84(n369)* L1 larvae (Johnson and Kramer, 2012). It would therefore be worthwhile to examine NE architecture in muscle tissues from human Emery–Dreifuss muscular dystrophy patients or mice with defective LINC complexes.

Human KASH and SUN luminal domains can replace *C. elegans* orthologues

The luminal domains of SUN proteins consist of the C-terminal SUN domain of ∼175 residues, a putative oligomerization domain next to the SUN domain, and a linker domain that connects the transmembrane domain at the INM to the oligomerization and SUN domains (Sosa et al., 2013). Although the SUN domain of UNC-84 is strongly conserved with human SUN1 and SUN2, the linker and oligomerization domains are poorly conserved (Malone et al., 1999; Tapley et al., 2011) However, we predicted that the function of linker and predicted oligomerization domains are conserved and that substitution of *C. elegans* KASH and SUN luminal domains with those from humans will still allow LINC complexes to carry out nuclear migration. To test this, we constructed transgenic worms that express chimeric KASH and SUN proteins in which the N-terminal nucleoplasmic/cytoplasmic domains of UNC-84 and UNC-83 were fused to the luminal domains of human SUN1 and Nesprin-4, which were chosen for functional homology (Fig. 3 A; Malone et al., 1999; Lei et al., 2009; Meyerzon et al., 2009; Roux et al., 2009). Because the luminal domains of KASH proteins are conserved, we predicted that expression of both chimeras should rescue the nuclear migration defect if the linker domain of SUN1 assumes a function sufficiently similar to that of UNC-84. The extent of normal nuclear migration in hyp7 cells was assayed by counting the number of hyp7 nuclei in the dorsal cord of L1 larvae, a readout for failed embryonic nuclear migration events (Fridolfsson et al., 2010). Indeed, in *unc-83; unc-84* double mutant animals, the UNC-84/SUN1 and UNC-83/Nesprin-4 KASH chimeric proteins rescued the nuclear migration defect (Fig. 3 B). Immunostaining confirmed that both chimeric proteins were properly localized to the NE (Fig. 3, C and C′). *C. elegans* can therefore function as a heterologous system to study the in vivo function of the luminal domains of human KASH and SUN proteins.

Human SUN2 assembles into a trimer via a noncanonical right-handed trimeric coiled coil in vitro to interact with three KASH peptides. A short, nonconserved region next to the conserved SUN domain is required for SUN2 trimerization in vitro (Sosa et al., 2012). We predicted that the human luminal domain of the chimeric UNC-84/SUN1 protein would similarly induce oligomerization in vivo and that oligomerization of the SUN protein is necessary for interaction with KASH domains. To test the necessity of the predicted trimerization domain, we deleted five amino acids (^{616}GITEA^{620} in full-length hSUN1) immediately upstream of the SUN domain. The UNC-84/SUN1(Δ616–620) chimera was expressed with the UNC-83/Nesprin-4 KASH chimeric protein in *unc-83; unc-84* double mutant animals. Although the mutant UNC-84/SUN1(Δ616–620) chimera properly localized to the NE (Fig. 3 D), it failed to recruit the KASH chimera to the ONM (Fig. 3 D′) and failed to rescue the nuclear migration phenotype of *unc-83; unc-84* mutant animals (Fig. 3 B). These results are consistent with the model that SUN proteins form oligomers in vivo and that oligomerization of the SUN protein is required for KASH binding and formation of LINC complexes.

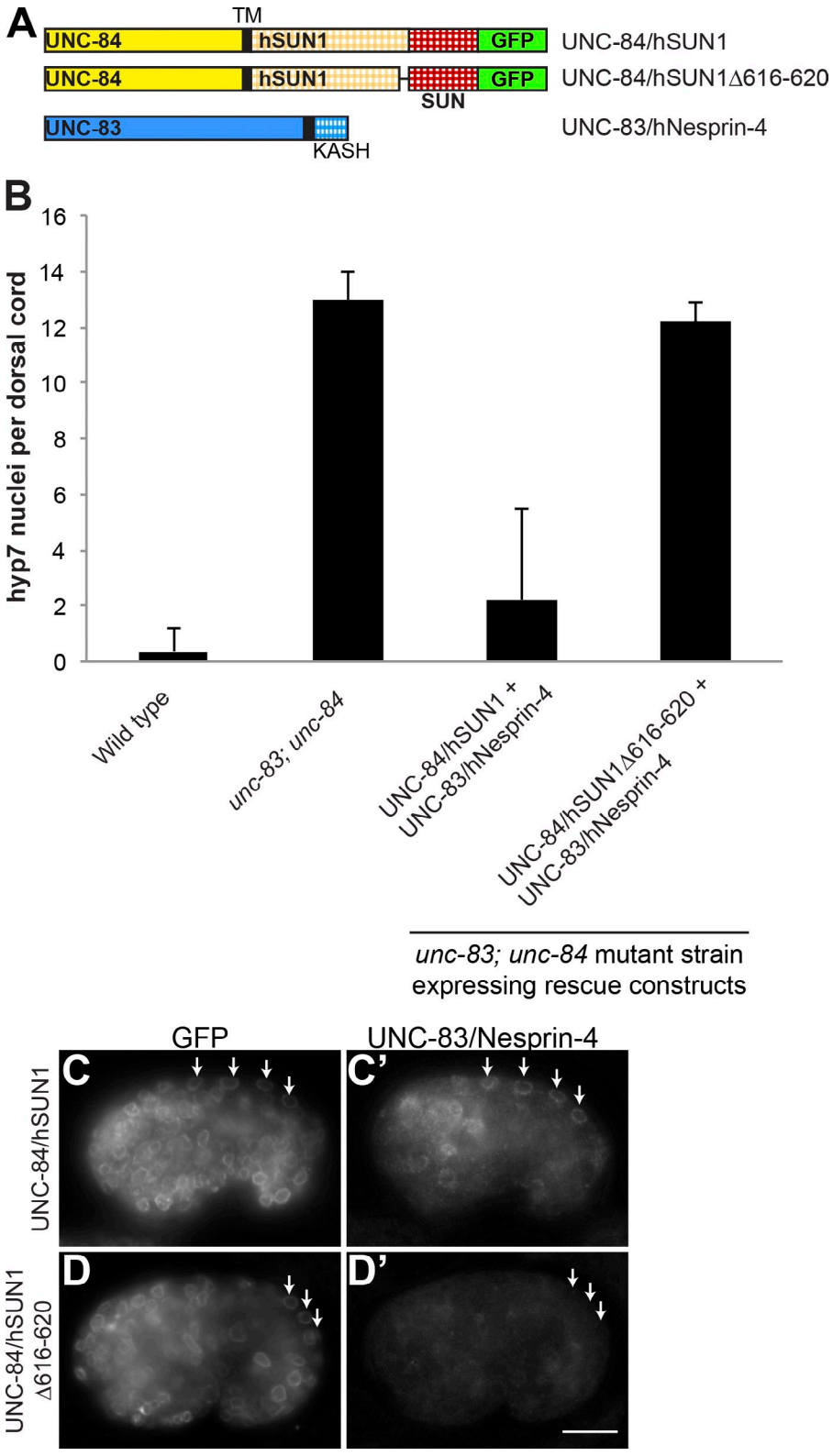

Figure 3. **Human KASH and SUN domains are functional for *C. elegans* hypodermal nuclear migration.** (A) Luminal domains of hSUN1 and Nesprin-4 (checkered shading) were fused to the nucleoplasmic and cytoplasmic domains of *C. elegans* UNC-84 and UNC-83 (solid shading), respectively. A C-terminal GFP was added to UNC-84/hSUN1 constructs. The transmembrane span (TM) is in black. (B) Mean number of dorsal cord nuclei in transgenic L1 larvae. Error bars denote standard deviations. For UNC-84/hSUN1(Δ616–620), three independent transgenic lines were assayed; data from one representative line are shown. (C and C') Immunofluorescence of transgenic *unc-84; unc*-83 double mutant embryos with anti-GFP and anti–UNC-83 antibodies showed that both chimeric proteins were localized to the NE. (D and D') Deletion of residues corresponding to 616–620 of the predicted trimerization domain of hSUN1 does not prevent localization of UNC-84/hSUN1 to the NE (D), but UNC-83/hNesprin-4 fails to localize (D'). Arrows indicate hyp7 nuclei that are positive for UNC-83 (C') or missing UNC-83 (D'). For all images, anterior is left, and dorsal is up. Bar, 10 µm.

Deletion analysis to identify functional domains in the luminal region of UNC-84

Having established that human luminal domains function in the *C. elegans* system, we sought to characterize the function of the predicted oligomerization and linker domains in UNC-84. UNC-84 has a single transmembrane helix at residues 512–532, and the C-terminal half of the protein (residues 533–1,111) resides in the PNS (Tapley et al., 2011). We previously showed that UNC-84 lacking the conserved SUN domain localizes to the INM but cannot recruit UNC-83 to the ONM or facilitate nuclear migration in hyp7 cells (McGee et al., 2006). Although coiled-coil prediction algorithms did not identify potential coiled-coil

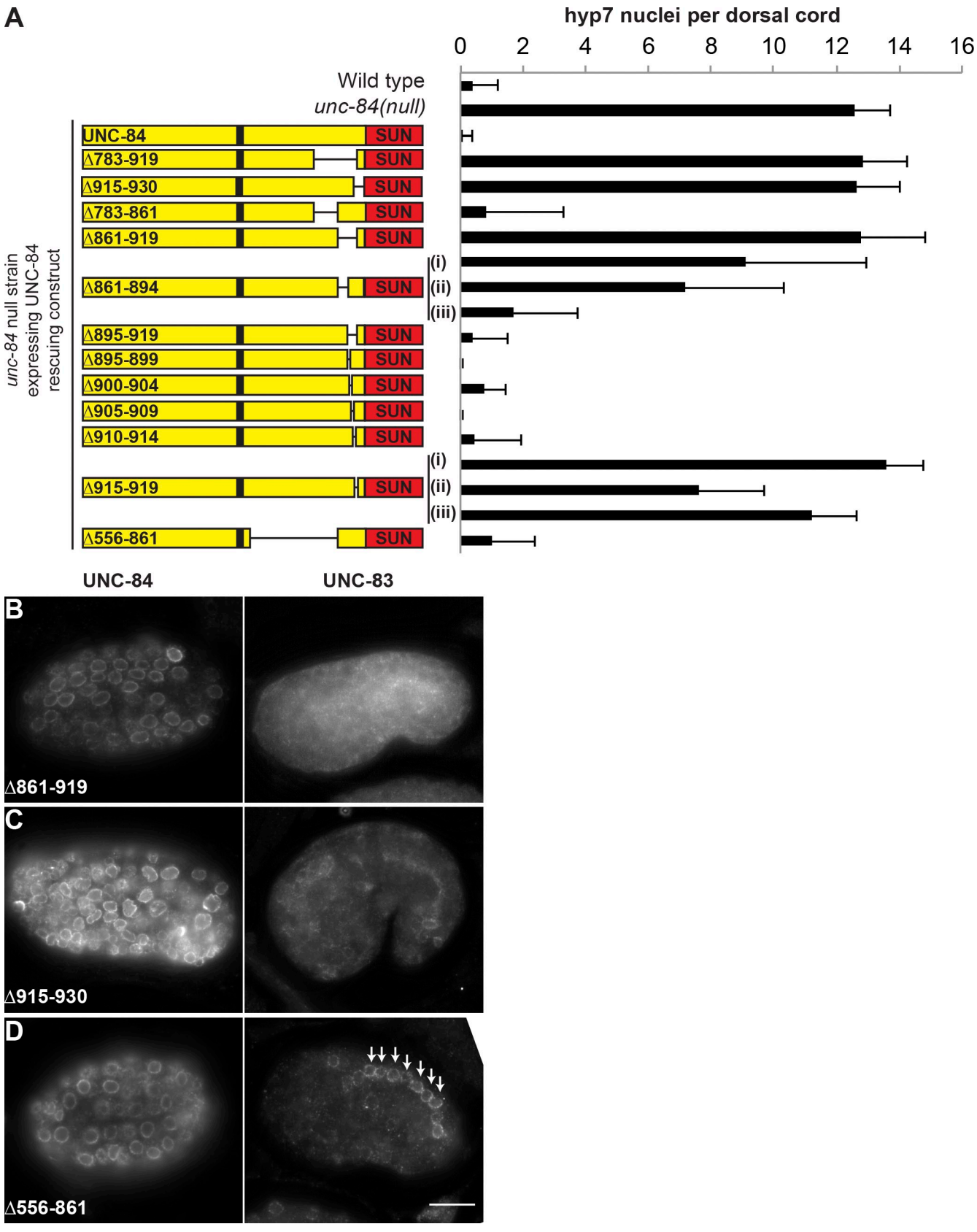

Figure 4. **Deletion analysis of the UNC-84 luminal domain.** (A) Schematics of the UNC-84 luminal domain deletions are presented along with the mean number of dorsal cord nuclei observed in L1 larva. Data for one representative line are shown for all deletions except *unc-84(Δ861–894)* and *unc-84(Δ915–919)*, both of which displayed varying means in three independent lines. Error bars denote standard deviations. (B–D) Transgenic *unc-84(n369)* mutant embryos expressing UNC-84 luminal domain deletion constructs were stained with anti–UNC-84 (left) and anti–UNC-83 (right) antibodies. *unc-84(Δ556–861)* retained the ability to recruit UNC-83 to the NE (D; arrows). For all images, anterior is left, and dorsal is up. Bar, 10 µm.

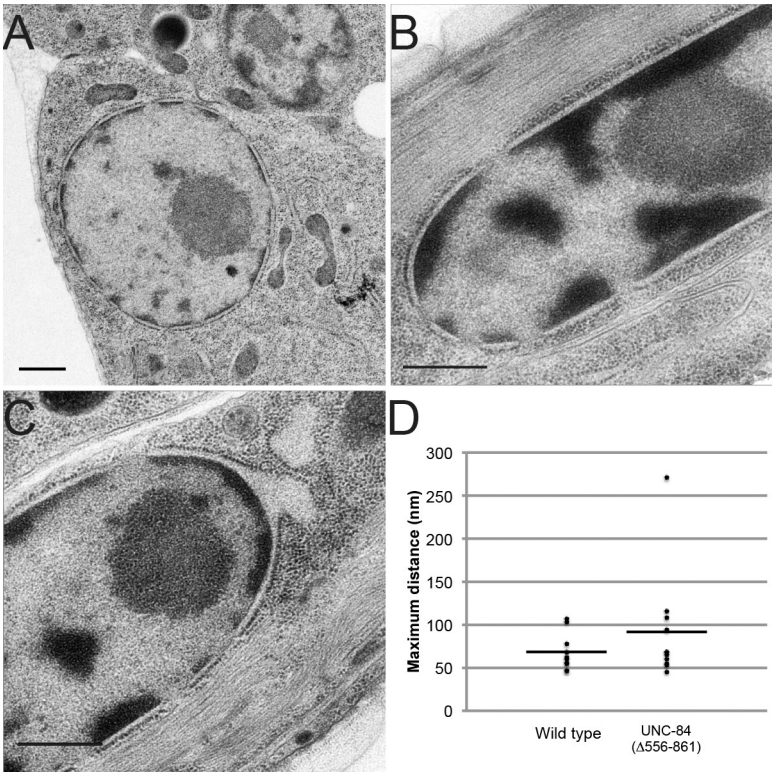

Figure 5. **Nuclei in *unc-84(Δ556–861)* embryos and larva do not display narrower NE spacing than wild type.** (A–C) TEM performed on *unc-84(n369)* transgenic nuclei expressing *unc-84(Δ556–861)* revealed that NE spacing in embryos (A) and muscle nuclei (B and C) were indistinguishable from wild type. Bars, 500 nm. (D) Quantitation of the maximum nuclear membrane distance confirmed that PNS widths in *unc-84(Δ556–861)* muscle cells were not significantly different than wild type (P = 0.2785). The horizontal bars denote the mean values.

domains in the linker domain (residues 533–936), as in mammalian SUN proteins (Padmakumar et al., 2005; Crisp et al., 2006), hydropathy analysis identified multiple regions of increased hydrophobicity, suggesting that the linker domain may assume some form of helical secondary structure.

To determine the regions of the luminal domain of UNC-84 required for function, we expressed a series of UNC-84 luminal deletions in *unc-84(n369)*–null animals (Fig. 4). We first tested the extent to which the region of UNC-84 just before the SUN domain was required for nuclear migration. We found that *unc-84(Δ861–919)* and *unc-84(Δ915–930)* failed to rescue nuclear migration (Fig. 4 A). Both constructs were expressed and localized to the NE but failed to recruit UNC-83 (Fig. 4, B and C). These data suggest that UNC-84(Δ861–919) and UNC-84(Δ915–930) are unable to interact with UNC-83, despite having intact SUN domains. Although most smaller deletions within residues 861–919 were functional, we observed only very slight rescue by *unc-84(Δ915–919)*. This result agrees with our data showing that a deletion of five amino acids near the SUN domain of the UNC-84/hSUN1 protein chimera (Fig. 3, B and D) also fails to rescue nuclear migration as well as with in vitro data showing that the region next to the conserved SUN domain functions in trimerization (Sosa et al., 2012). We next focused on the residues between the transmembrane span and the trimerization domain. Surprisingly, UNC-84(Δ556–861), a deletion of 306 amino acids of the luminal domain of UNC-84, was able to recruit UNC-83 to the ONM (Fig. 4 D) and to completely rescue the *unc-84(n369)* nuclear migration defect. We therefore concluded that most of the luminal domain of UNC-84 is dispensable for function, but trimerization, or some form of oligomerization, of SUN proteins is functionally important in vivo during nuclear migration.

Shortening SUN proteins had no effect on NE spacing

We predicted that the function of UNC-84(Δ556–861) would require a shrinking of the PNS to allow its interaction with KASH proteins in the ONM. To test this hypothesis, we performed TEM on *unc-84(n369)*–null animals expressing the UNC-84(Δ556–861) rescue fragment from an integrated site in the genome. NE ultrastructure was examined in multiple *C. elegans* embryonic and L1 tissues. Although we did not observe NE distortions in the *unc-84(null)* embryos (Fig. 1), we hypothesized that if the length of UNC-84 defines the PNS, a noticeable narrowing of the space surrounding nuclei would be observed in UNC-84(Δ556–861) embryos. However, the PNS width in UNC-84(Δ556–861) embryonic nuclei appeared comparable to that in wild-type embryos (n = 47; Fig. 5 A). To better quantify our data, we focused on the ends of L1 body wall muscle nuclei as in Fig. 2. Most muscle nuclei had normal NE spacing (Fig. 5 B), whereas one displayed a wider PNS similar to the *unc-84(n369)* mutant (Fig. 5 C). In this nucleus, we suspect that LINC complexes were either absent or may have been severed.

Quantification of the PNS distance in UNC-84(Δ556–861) nuclei confirmed that NE spacing was not narrower than that of wild type. The maximum separation ranged from 44.9 to 271.5 nm, with a mean of 91.3 nm. When compared with wild type, a two–tailed unpaired t test with Welch's correction gave a P = 0.28, indicating that the difference between the two strains is not significant. These results suggest that despite its shorter size, UNC-84(Δ556–861) is capable of maintaining the normal distance between the INM and ONM.

There are two possibilities for how UNC-84(Δ556–861) might recruit UNC-83 and function in nuclear migration without

observably narrowing the PNS. First, it is possible that UNC-84(Δ556–861) causes PNS shrinking only in discrete locations. It is not known how many UNC-84/UNC-83 bridges are required for nuclear migration. Perhaps only a few per nucleus are required, too few to resolve with our high pressure freezing conditions. Alternatively, the remaining residues in the linker domain of the UNC-84(Δ556–861) mutant could be fully extended. Approximately 60 residues remain between the transmembrane span and the oligomerization domain in the UNC-84(Δ556–861) mutant. A fully extended peptide is predicted to be 3.8 Å per residue. A fully extended peptide could hypothetically extend 20–25 nm. The two lipid bilayers (5 nm each) and the globular SUN domain (4 nm; Sosa et al., 2012) may add an additional 14 nm. Thus, the fully extended linker, SUN domain, and nuclear membranes could account for the observed distances in body wall muscle nuclei (Fig. 5 D). Nonetheless, the data presented here suggest that LINC complexes do not function to dictate the width of the PNS.

If not LINC complexes, what sets the even spacing of the PNS between nuclear pore complexes? We propose that the spacing of nuclear membranes is an inherent property of rough ER membranes. It is reasonable to predict that membranes associated with heterochromatin (the INM) or polyribosomes (the ONM and the rough ER) have external pressures to remain flat (Puhka et al., 2007). These forces would prevent blebbing between the INM and ONM in all nuclei except those under extreme mechanical strain, such as adherent tissue-culture cells or *C. elegans* body wall muscle cells. The best candidate to maintain the flat and even spacing in ER sheets is Climp63, a transmembrane protein in the ER with luminal, coiled-coil domains. However, siRNA knockdown of Climp63 did not cause ER sheets to bleb. Instead, Climp63 siRNA–treated ER sheets remain flat and actually become narrower than wild-type ER sheets, approximately the width of the NE in normal cells (Shibata et al., 2010). We therefore propose that ER sheets lacking Climp63 collapse to a thinner sheet that is dictated by inherent properties of rough ER membranes. Our data are consistent with this model; the LINC complex is dispensable for NE morphology in most cells. In our model, SUN proteins have evolved to reach across the PNS, rather than to dictate the width of the PNS.

Materials and methods

C. elegans strains, maintenance, and phenotypic characterization

C. elegans were cultured on nematode growth medium plates seeded with OP50 bacteria and maintained at 15°C. The N2 strain was used for wild-type controls (Brenner, 1974). The null alleles *unc-83(e1408)* (W904Stop) and *unc-84(n369)* (W88Stop) were previously described (Horvitz and Sulston, 1980; Malone et al., 1999; Starr et al., 2001). Some strains were provided by the Caenorhabditis Genetics Center, which is supported by the National Institutes of Health National Center for Research Resources.

Transgenic lines were created (Table S1) using standard DNA microinjection techniques using 2–4 ng/µl of the construct of interest and 100 ng/µl of the injection marker construct (either the full-length translational *sur-5::GFP* fusion construct or the transcriptional $p_{odr\text{-}1}$*::GFP* construct; Mello et al., 1991; Gu et al., 1998; L'Etoile and Bargmann, 2000). Chimeric SUN and KASH proteins were expressed together in *unc-83(e1408); unc-84(n369)* double mutant animals. Deletion analysis of UNC-84 was performed by expressing truncated UNC-84 constructs in the *unc-84(n369)* background. UD87, expressing the full-length UNC-84 rescue construct, was used as a positive control (McGee et al., 2006; Chang et al., 2013). Integration of the *unc-84(556–861)* extrachromosomal array was performed by γ irradiation of L4 animals with a ^{137}cesium source (University of California, Davis Center for Health and the Environment) and selection for 100% of F3 progeny expressing the injection marker (Evans, 2006) to make the strain UD177, *n369 ycIs13[unc-84(Δ556–861); sur-5::gfp]*.

Hyp7 nuclear migration was assayed by counting dorsal cord nuclei of L1 larvae in M9 buffer with 1 mM tetramisole (MP Biomedicals) at room temperature using differential interference contrast (DIC) microscopy with a HCX Plan Apochromat 63×, 1.40 NA objective on a compound microscope (DM6000; Leica) with AF6000 software (Leica) as previously described (Meyerzon et al., 2009). At least 15 animals were scored for each genotype. Failure to rescue the null phenotype of *unc-84(n369)* or *unc-83(e1408); unc-84(n369)* was confirmed in three independent transgenic lines for each construct. All counts were performed blind, i.e., dorsal nuclei were counted by DIC before identifying each animal as transgenic or nontransgenic by fluorescence.

UNC-83 and UNC-84 mutant transgenic constructs

To create pSL549, which encodes the UNC-84/hSUN1 chimeric protein, a PCR fragment containing the luminal domain of hSUN1 was amplified from cDNA KIAA0810 (Suyama et al., 1999) and subcloned into pSL226, which contains 2.2 kb of endogenous UNC-84 promoter sequence, followed by genomic sequence encoding the nucleoplasmic domain (residues 1–535) fused in frame to GFP (Tapley et al., 2011). The hSUN1 PCR fragment was then inserted between the transmembrane domain of UNC-84 and the C-terminal GFP tag. pSL577, the UNC-84/hSUN1(Δ616–620) construct, was made using PCR splicing by overlap extension (Horton et al., 1990). The fusion PCR fragment containing the deletion was cloned into a TOPO vector (Life Technologies) and subcloned into pSL549. To construct pSL567, encoding the UNC-83/Nesprin-4 chimeric protein, the transmembrane and KASH domains of Nesprin-4 were amplified from cDNA C19orf46 (OriGene) and introduced into pSL61, a version of the UNC-83–rescuing construct pDS22 (Starr et al., 2001), in which the transmembrane and KASH domains of UNC-83 were deleted and replaced with a NotI site. UNC-84 deletion alleles were introduced into the UNC-84–rescuing construct pSL38 (McGee et al., 2006) by PCR splicing by overlap extension as described for pSL577 or one-step isothermal DNA assembly (Gibson et al., 2009).

Antibodies and immunofluorescence of *C. elegans* embryos

For localization of UNC-84 in embryos, a new monoclonal antibody against the N terminus of UNC-84 (synthetic peptide ^{5}TEADNNFDTHEWKSE^{19}) was raised in BALB/c mice. Mice were injected with a keyhole limpet hemocyanin–conjugated peptide, and splenocytes from one mouse were used to generate hybridomas by standard procedures (Trimmer et al., 1985). Screening by ELISA against BSA-conjugated peptide resulted in identification of three clones (L72/1, L72/6, and L72/13) that were also positive by immunofluorescence labeling of *C. elegans* embryos. All three clones were subcloned by limiting dilution. For further experiments, tissue-culture supernatants from clone L72/6 (isotype IgM) were used at a 1:100 dilution in PBS with 0.1% Triton X-100 for immunostaining. A tissue-culture supernatant for mouse monoclonal anti–UNC-83 line 1209D7D5 (Starr et al., 2001) was used undiluted. Rabbit polyclonal antibody NB600-308 against GFP (Novus Biologicals) was diluted 1:200 in UNC-83 antiserum for simultaneous staining of KASH and SUN chimeric proteins. Secondary antibodies used were as follows: Cy3-conjugated goat anti–mouse IgG diluted 1:200 (Jackson ImmunoResearch Laboratories, Inc.) and Alexa Fluor antibodies 555 goat anti–mouse IgM, 488 goat anti–rabbit IgG, and 594 goat anti–mouse IgG diluted 1:500 (Life Technologies). DNA was stained with 1 µg/ml DAPI for 10 min.

To visualize UNC-83 and UNC-84, *C. elegans* embryos were extruded from gravid hermaphrodites and fixed as previously described (Starr et al., 2001; McGee et al., 2006; Fridolfsson et al., 2010). For both UNC-83 and UNC-84 staining, embryos were fixed in −20°C methanol for 10 min. Embryos were then stained with undiluted mouse monoclonal UNC-83 antiserum or 1:100 diluted mouse UNC-84 antibody as described in the previous paragraph. Fixed and stained embryos were mounted in 90% glycerol and 10% PBS with 1% DABCO (Sigma Aldrich) and imaged at room temperature. Images were captured with a HCX Plan Apochromat 63, 1.40 NA objective on a compound microscope (DM6000) with AF6000 software. Images were uniformly enhanced using the background subtraction and brightness/contrast commands in ImageJ (National Institutes of Health; Schneider et al., 2012).

Locomotion assays of L1 larvae

L1 larvae were imaged in 10 µl of M9 buffer (Brenner, 1974) at room temperature on a microscope slide without a coverslip with a HC Plan Apochromat 10×, 0.4 NA objective on a compound microscope (DM6000) with

a camera (LDFC350FX; Leica) at a frame rate of 16.2 frames per second (fps) for 30 s. Head thrashes were counted manually from playback of each video, with one head thrash defined as a complete change in direction from the starting point of the head. Animals were assayed blind, in that the strain identity was hidden both at the time of capture and at the time of counting.

For motion spectrum analysis, each video was cropped to 253 × 253 pixels to center on the animal, which was located using the maximum intensity pixel in each frame. To prevent introduction of high frequency noise, a Gaussian window function with a standard deviation of 3.0 time steps was used to smooth the center location frame to frame. Each frame was flat field corrected to reduce the effect of uneven illumination from the light source. To isolate the locomotion signal for our analysis, we used a covariance principle component decomposition similar to Buckingham and Sattelle (2009) with modifications. We transformed each processed video from an N_x by N_y by N_{time} data cube into an N_{pixel} by N_{time} matrix. Each row of the matrix was Fourier transformed and used to generate a power spectrum (in arbitrary units) for each pixel. This gives an N_{pixel} by N_{freq} matrix (in which $N_{freq} = N_{time} = 500$) with which we constructed the frequency-wise covariance matrix that was then decomposed into its principal components. The first 10 principal components were used to characterize the motion of each animal. We calculated the scalar product between each pixel's spectrum and each of the first 10 principal components. We calculated the mean and variance of these scalar products and used them, along with the principal components, to construct a mean spectrum and its variance for each video. We summed the mean spectra of all videos for each strain and likewise computed the combined variance at each frequency. For clarity, we renormalized the mean combined spectrum for each strain. All analysis was performed in Python using Canopy version 1.4 (Enthought).

EM of *C. elegans* embryos and larvae

TEM of high pressure frozen *C. elegans* embryos and L1 larvae was performed using previously described techniques (McDonald, 2007, 2014; McDonald and Webb, 2011) In brief, worms were frozen in 50-µm-deep specimen carriers in a high pressure freezer (HPM 010; Bal-Tec), freeze substituted in 1% osmium tetroxide plus 0.1% uranyl acetate in acetone over 2.5 h (McDonald and Webb, 2011), and embedded in Epon-Araldite resin over a period of 2.5 h (McDonald, 2014). 70-nm-thick serial sections were picked up on slot grids, poststained with uranyl acetate and lead citrate, and imaged either in a transmission electron microscope (Tecnai 12; FEI) operating at 120 kV with a charge-coupled device camera (Gatan UltraScan; University of California, Berkeley Electron Microscope Laboratory) or with a 2,048 × 2,048 charge-coupled device camera (Tietz F214; TVIPS) on a microscope (JEM 1230; JEOL) operating at 100 kV (University of California, Davis Electron Imaging Facility). Measurements of NE spacing were taken by counting pixels with the ruler tool in Photoshop (Adobe) and converting to nanometers using calibrated nanometer/pixel ratios. At least 10 muscle nuclei were observed for each genotype, and at least five serial sections were measured per nucleus.

Online supplemental material

Table S1 lists the transgenic strains generated for this study. Video 1 shows a representative DIC video of one wild-type L1 larva thrashing with regular rhythm in M9 buffer for 30 s, as in Fig. 2 G. Video 2 shows a representative DIC video of one *unc-84(n369)* larva thrashing with twitches and coils in M9 buffer for 30 s as in Fig. 2 H. Online supplemental material is available at http://www.jcb.org/cgi/content/full/jcb.201405081/DC1.

We thank James Trimmer and Ashleigh Evans at the University of California, Davis (UC Davis)/National Institutes of Health NeuroMab facility for assistance making the UNC-84 monoclonal antibody and Ruben Diaz-Avalos at the College of Biological Sciences UC Davis electron imaging facility for assistance with EM imaging. We thank John Yochem for assistance in cell identification, David Fay and Dan Levy (University of Wyoming) for helpful discussions and hosting D.A. Starr on sabbatical. We thank Zi Mei Jiang and Gavin Rice (UC Davis) for technical assistance. We thank Thomas Schwartz (Massachusetts Institute of Technology), Ulrike Kutay (Zurich), Kelly Liu (Cornell University), the members of the Starr laboratory, and our colleagues in the Department of Molecular and Cellular Biology at UC Davis for helpful discussions.

This study was supported by a postdoctoral fellowship from the American Cancer Society, Illinois Division PF-13-094-01-CGC (to N.E. Cain) and by grant R01 GM073874 from the National Institutes of Health/National Institute of General Medical Sciences (to D.A. Starr).

The authors declare no competing financial interests.

Submitted: 22 May 2014
Accepted: 12 June 2014

References

Altun, Z.F., and D.H. Hall. 2009. Muscle system, somatic muscle. *WormAtlas*. http://dx.doi.org/10.3908/wormatlas.1.7

Azibani, F., A. Muchir, N. Vignier, G. Bonne, and A.T. Bertrand. 2014. Striated muscle laminopathies. *Semin. Cell Dev. Biol.* 29:107–115. http://dx.doi.org/10.1016/j.semcdb.2014.01.001

Brenner, S. 1974. The genetics of *Caenorhabditis elegans*. *Genetics*. 77:71–94. PubMed

Buckingham, S.D., and D.B. Sattelle. 2009. Fast, automated measurement of nematode swimming (thrashing) without morphometry. *BMC Neurosci.* 10:84. http://dx.doi.org/10.1186/1471-2202-10-84

Chang, Y.T., D. Dranow, J. Kuhn, M. Meyerzon, M. Ngo, D. Ratner, K. Warltier, and D.A. Starr. 2013. toca-1 is in a novel pathway that functions in parallel with a SUN-KASH nuclear envelope bridge to move nuclei in *Caenorhabditis elegans*. *Genetics*. 193:187–200. http://dx.doi.org/10.1534/genetics.112.146589

Cohen, M., Y.B. Tzur, E. Neufeld, N. Feinstein, M.R. Delannoy, K.L. Wilson, and Y. Gruenbaum. 2002. Transmission electron microscope studies of the nuclear envelope in *Caenorhabditis elegans* embryos. *J. Struct. Biol.* 140:232–240. http://dx.doi.org/10.1016/S1047-8477(02)00516-6

Crisp, M., Q. Liu, K. Roux, J.B. Rattner, C. Shanahan, B. Burke, P.D. Stahl, and D. Hodzic. 2006. Coupling of the nucleus and cytoplasm: role of the LINC complex. *J. Cell Biol.* 172:41–53. http://dx.doi.org/10.1083/jcb.200509124

Evans, T.C. 2006. Transformation and microinjection. *WormBook*. http://dx.doi.org/10.1895/wormbook.1.108.1

Franke, W.W., U. Scheer, G. Krohne, and E.D. Jarasch. 1981. The nuclear envelope and the architecture of the nuclear periphery. *J. Cell Biol.* 91:39s–50s. http://dx.doi.org/10.1083/jcb.91.3.39s

Fridkin, A., E. Mills, A. Margalit, E. Neufeld, K.K. Lee, N. Feinstein, M. Cohen, K.L. Wilson, and Y. Gruenbaum. 2004. Matefin, a *Caenorhabditis elegans* germ line-specific SUN-domain nuclear membrane protein, is essential for early embryonic and germ cell development. *Proc. Natl. Acad. Sci. USA*. 101:6987–6992. http://dx.doi.org/10.1073/pnas.0307880101

Fridolfsson, H.N., N. Ly, M. Meyerzon, and D.A. Starr. 2010. UNC-83 coordinates kinesin-1 and dynein activities at the nuclear envelope during nuclear migration. *Dev. Biol.* 338:237–250. http://dx.doi.org/10.1016/j.ydbio.2009.12.004

Gibson, D.G., L. Young, R.Y. Chuang, J.C. Venter, C.A. Hutchison III, and H.O. Smith. 2009. Enzymatic assembly of DNA molecules up to several hundred kilobases. *Nat. Methods*. 6:343–345. http://dx.doi.org/10.1038/nmeth.1318

Gu, T., S. Orita, and M. Han. 1998. *Caenorhabditis elegans* SUR-5, a novel but conserved protein, negatively regulates LET-60 Ras activity during vulval induction. *Mol. Cell. Biol.* 18:4556–4564.

Horton, R.M., Z.L. Cai, S.N. Ho, and L.R. Pease. 1990. Gene splicing by overlap extension: tailor-made genes using the polymerase chain reaction. *Biotechniques*. 8:528–535.

Horvitz, H.R., and J.E. Sulston. 1980. Isolation and genetic characterization of cell-lineage mutants of the nematode *Caenorhabditis elegans. Genetics*. 96:435–454.

Johnson, R.P., and J.M. Kramer. 2012. Neural maintenance roles for the matrix receptor dystroglycan and the nuclear anchorage complex in *Caenorhabditis elegans*. *Genetics*. 190:1365–1377. http://dx.doi.org/10.1534/genetics.111.136184

Lee, K.K., D. Starr, M. Cohen, J. Liu, M. Han, K.L. Wilson, and Y. Gruenbaum. 2002. Lamin-dependent localization of UNC-84, a protein required for nuclear migration in *Caenorhabditis elegans*. *Mol. Biol. Cell*. 13:892–901. http://dx.doi.org/10.1091/mbc.01-06-0294

Lei, K., X. Zhang, X. Ding, X. Guo, M. Chen, B. Zhu, T. Xu, Y. Zhuang, R. Xu, and M. Han. 2009. SUN1 and SUN2 play critical but partially redundant roles in anchoring nuclei in skeletal muscle cells in mice. *Proc. Natl. Acad. Sci. USA*. 106:10207–10212. http://dx.doi.org/10.1073/pnas.0812037106

L'Etoile, N.D., and C.I. Bargmann. 2000. Olfaction and odor discrimination are mediated by the *C. elegans* guanylyl cyclase ODR-1. *Neuron*. 25:575–586. http://dx.doi.org/10.1016/S0896-6273(00)81061-2

Li, P., P. Meinke, T.T. Huong, M. Wehnert, and A.A. Noegel. 2014. Contribution of SUN1 mutations to the pathomechanism in muscular dystrophies. *Hum. Mutat.* 35:452–461. http://dx.doi.org/10.1002/humu.22504

Magidson, V., C.B. O'Connell, J. Lončarek, R. Paul, A. Mogilner, and A. Khodjakov. 2011. The spatial arrangement of chromosomes during prometaphase facilitates spindle assembly. *Cell*. 146:555–567. http://dx.doi.org/10.1016/j.cell.2011.07.012

Malone, C.J., W.D. Fixsen, H.R. Horvitz, and M. Han. 1999. UNC-84 localizes to the nuclear envelope and is required for nuclear migration and anchoring during *C. elegans* development. *Development*. 126:3171–3181.

McDonald, K. 2007. Cryopreparation methods for electron microscopy of selected model systems. *Methods Cell Biol.* 79:23–56. http://dx.doi.org/10.1016/S0091-679X(06)79002-1

McDonald, K.L. 2014. Rapid embedding methods into epoxy and LR White resins for morphological and immunological analysis of cryofixed biological specimens. *Microsc. Microanal.* 20:152–163. http://dx.doi.org/10.1017/S1431927613013846

McDonald, K.L., and R.I. Webb. 2011. Freeze substitution in 3 hours or less. *J. Microsc.* 243:227–233. http://dx.doi.org/10.1111/j.1365-2818.2011.03526.x

McGee, M.D., R. Rillo, A.S. Anderson, and D.A. Starr. 2006. UNC-83 IS a KASH protein required for nuclear migration and is recruited to the outer nuclear membrane by a physical interaction with the SUN protein UNC-84. *Mol. Biol. Cell.* 17:1790–1801. http://dx.doi.org/10.1091/mbc.E05-09-0894

Mello, C.C., J.M. Kramer, D. Stinchcomb, and V. Ambros. 1991. Efficient gene transfer in *C. elegans*: extrachromosomal maintenance and integration of transforming sequences. *EMBO J.* 10:3959–3970.

Meyerzon, M., H.N. Fridolfsson, N. Ly, F.J. McNally, and D.A. Starr. 2009. UNC-83 is a nuclear-specific cargo adaptor for kinesin-1-mediated nuclear migration. *Development*. 136:2725–2733. http://dx.doi.org/10.1242/dev.038596

Minn, I.L., M.M. Rolls, W. Hanna-Rose, and C.J. Malone. 2009. SUN-1 and ZYG-12, mediators of centrosome-nucleus attachment, are a functional SUN/KASH pair in *Caenorhabditis elegans*. *Mol. Biol. Cell*. 20:4586–4595. http://dx.doi.org/10.1091/mbc.E08-10-1034

Padmakumar, V.C., T. Libotte, W. Lu, H. Zaim, S. Abraham, A.A. Noegel, J. Gotzmann, R. Foisner, and I. Karakesisoglou. 2005. The inner nuclear membrane protein Sun1 mediates the anchorage of Nesprin-2 to the nuclear envelope. *J. Cell Sci.* 118:3419–3430. http://dx.doi.org/10.1242/jcs.02471

Puckelwartz, M.J., E.J. Kessler, G. Kim, M.M. Dewitt, Y. Zhang, J.U. Earley, F.F. Depreux, J. Holaska, S.K. Mewborn, P. Pytel, and E.M. McNally. 2010. Nesprin-1 mutations in human and murine cardiomyopathy. *J. Mol. Cell. Cardiol.* 48:600–608. http://dx.doi.org/10.1016/j.yjmcc.2009.11.006

Puhka, M., H. Vihinen, M. Joensuu, and E. Jokitalo. 2007. Endoplasmic reticulum remains continuous and undergoes sheet-to-tubule transformation during cell division in mammalian cells. *J. Cell Biol.* 179:895–909. http://dx.doi.org/10.1083/jcb.200705112

Roux, K.J., M.L. Crisp, Q. Liu, D. Kim, S. Kozlov, C.L. Stewart, and B. Burke. 2009. Nesprin 4 is an outer nuclear membrane protein that can induce kinesin-mediated cell polarization. *Proc. Natl. Acad. Sci. USA*. 106:2194–2199. http://dx.doi.org/10.1073/pnas.0808602106

Schneider, C.A., W.S. Rasband, and K.W. Eliceiri. 2012. NIH Image to ImageJ: 25 years of image analysis. *Nat. Methods*. 9:671–675. http://dx.doi.org/10.1038/nmeth.2089

Shibata, Y., T. Shemesh, W.A. Prinz, A.F. Palazzo, M.M. Kozlov, and T.A. Rapoport. 2010. Mechanisms determining the morphology of the peripheral ER. *Cell*. 143:774–788. http://dx.doi.org/10.1016/j.cell.2010.11.007

Sosa, B.A., A. Rothballer, U. Kutay, and T.U. Schwartz. 2012. LINC complexes form by binding of three KASH peptides to domain interfaces of trimeric SUN proteins. *Cell.* 149:1035–1047. http://dx.doi.org/10.1016/j.cell.2012.03.046

Sosa, B.A., U. Kutay, and T.U. Schwartz. 2013. Structural insights into LINC complexes. *Curr. Opin. Struct. Biol.* 23:285–291. http://dx.doi.org/10.1016/j.sbi.2013.03.005

Starr, D.A., and H.N. Fridolfsson. 2010. Interactions between nuclei and the cytoskeleton are mediated by SUN-KASH nuclear-envelope bridges. *Annu. Rev. Cell Dev. Biol.* 26:421–444. http://dx.doi.org/10.1146/annurev-cellbio-100109-104037

Starr, D.A., and M. Han. 2002. Role of ANC-1 in tethering nuclei to the actin cytoskeleton. *Science*. 298:406–409. http://dx.doi.org/10.1126/science.1075119

Starr, D.A., G.J. Hermann, C.J. Malone, W. Fixsen, J.R. Priess, H.R. Horvitz, and M. Han. 2001. unc-83 encodes a novel component of the nuclear envelope and is essential for proper nuclear migration. *Development*. 128:5039–5050.

Suyama, M., T. Nagase, and O. Ohara. 1999. HUGE: a database for human large proteins identified by Kazusa cDNA sequencing project. *Nucleic Acids Res.* 27:338–339. http://dx.doi.org/10.1093/nar/27.1.338

Tapley, E.C., N. Ly, and D.A. Starr. 2011. Multiple mechanisms actively target the SUN protein UNC-84 to the inner nuclear membrane. *Mol. Biol. Cell*. 22:1739–1752. http://dx.doi.org/10.1091/mbc.E10-08-0733

Trimmer, J.S., I.S. Trowbridge, and V.D. Vacquier. 1985. Monoclonal antibody to a membrane glycoprotein inhibits the acrosome reaction and associated Ca2+ and H+ fluxes of sea urchin sperm. *Cell*. 40:697–703. http://dx.doi.org/10.1016/0092-8674(85)90218-1

Wang, N., J.D. Tytell, and D.E. Ingber. 2009a. Mechanotransduction at a distance: mechanically coupling the extracellular matrix with the nucleus. *Nat. Rev. Mol. Cell Biol.* 10:75–82. http://dx.doi.org/10.1038/nrm2594

Wang, X., Y. Zhao, K. Wong, P. Ehlers, Y. Kohara, S.J. Jones, M.A. Marra, R.A. Holt, D.G. Moerman, and D. Hansen. 2009b. Identification of genes expressed in the hermaphrodite germ line of *C. elegans* using SAGE. *BMC Genomics*. 10:213. http://dx.doi.org/10.1186/1471-2164-10-213

Worman, H.J. 2012. Nuclear lamins and laminopathies. *J. Pathol.* 226:316–325. http://dx.doi.org/10.1002/path.2999

Zhang, J., A. Felder, Y. Liu, L.T. Guo, S. Lange, N.D. Dalton, Y. Gu, K.L. Peterson, A.P. Mizisin, G.D. Shelton, et al. 2010. Nesprin 1 is critical for nuclear positioning and anchorage. *Hum. Mol. Genet.* 19:329–341. http://dx.doi.org/10.1093/hmg/ddp499